On-line State of Health Estimation of VRLA Batteries Using State of Charge

Abstract: This paper presents an on-line method for estimation of the State of Health (SOH) of Valve-Regulated Lead-Acid (VRLA) batteries. The proposed method is based on the State of Charge (SOC) of the battery. The SOC is estimated using the extended Kalman filter and a neural network model of the battery. Then, the SOH is estimated on-line based on the relationship between the SOC and the battery open-circuit voltage using the fuzzy logic and the recursive least square method. In order to obtain the open-circuit voltage while the battery is connected to the system, the reflective charging process is employed. Experimental results show good on-line estimation of the SOH of VRLA batteries.

Keywords: Batteries, monitoring, state estimation.

1. INTRODUCTION

Batteries play fundamental role in energy-storing and back-up supply systems. One important issue in utilization of rechargeable batteries is this question: How many times a battery can be charged and discharged while supplying the required power? The answer to this question is known as the State of Health (SOH). One reason for deterioration of the SOH is that batteries age, resulting in higher internal resistances and higher terminal voltages. The SOH is important due to the following reasons:

- Optimal usage and better management of the battery in important equipments
- Determining the precise time for battery replacement in sensitive applications
- Identifying the bad cell in a bank of batteries
- Determining the required power for the task
- Better selection of batteries by the user
- Determining the life expectancy and reliability of batteries as a reserve power source in an uninterrupted power supply in the case of AC power failure

Different methods have been proposed by researchers to determine the SOH of batteries. These methods take advantage of various characteristics and parameters of batteries such as electrochemical properties, electrical variables (i.e. terminal current and voltage), and State of Charge (SOC).

Meissner and Richter have shown the relation between the Battery Management System (BMS) and algorithms for defining different states of batteries such as SOC and SOH [1]. They define a simple equation for the SOC as $\mathrm{SOC} = 1 - \mathrm{DOD}$, where DOD stands for the Depth of Discharge. Szumanowski and Chang have modeled the battery based on its discharge and charge characteristics under different constant currents and have determined the battery SOC according to this battery modeling [2]. Divakar *et al.* have proposed a model for the BMS, where one of its states is the SOC, which is calculated using the Ampere-hour counting technique. In their method, other parameters of the battery such as SOH can be extracted [3]. Pattipati *et al.* have defined several tasks for the BMS such as protecting the cell, controlling the charge, and determining SOC, SOH, and the Remaining Useful Life (RUL), cell balancing, and monitoring and storing historical data [4]. Kaiser has shown the relation between BMS and SOC, SOH, and DOD. Analysis of SOC and SOH helps for better management of the charge and discharge of batteries [5]. Wong *et al.* has defined appropriate regimes for the standby charge control of Valve-Regulated Lead-Acid (VRLA) batteries by analyzing its service life [6].

Salkind *et al.* modeled VRLA batteries based on the electrochemical properties and the voltage and current during charging and discharging processes [7]. In this row, Pascoe and Anbuky have proposed a different model based on the rate of charge, the environment temperature, the initial SOC, and the decay of SOH of VRLA batteries [8]. Jossen has developed this model based on more characteristics of the battery [9]. These papers describe basic dynamical characteristics of batteries in the frequency range from some mHz up to several MHz, and explain that the dynamical behavior of batteries depend on their SOC and SOH. Jossen has expressed that the dynamical behavior of batteries is influenced by both the internal and external parameters. According to his definitions, internal parameters are SOC, SOH, AC and DC resistances, and the battery design parameters. On the other hand, external parameters are the temperature, the DC current, and the short- and long-term histories. Damlund [10], Cox and Perez-Kite [11], and Pasco and Anbuky [12] showed the effective parameters on the SOH. Damlund proposed two AC measuring methods for the impedance and

conductance tests for determining the SOH; both methods are useful in identifying bad cells in battery-strings connected in series or parallel. Pascoe and Anbuky proposed an algorithm for estimating the SOH based on the battery temperature and the coup-de-fouet parameters. They showed that temperature rise in a battery has a low-to-medium reliability on the SOH of VRLA batteries. The temperature often rises considerably only after the SOH has decreased dramatically.

Bose and Beaird showed that coup-de-fouet parameters have linear relation with the SOH of VRLA batteries [13]. Later, Pascoe and Anbuky showed this linear relation more comprehensively [14]. Delaille *et al.* studied the coup de fouet as a function of SOH and SOC for lead-acid batteries [15]. Based on the definition of coup de fouet, this parameter can be used only for the first 3 to 5 minutes of the discharging process when the battery is completely charged. Therefore, this method cannot be used in different conditions. In 2005, Blanke *et al.* have used impedance measurement to asses the SOC and SOH of lead-acid batteries [16]. Kiel *et al.* have showed that certain aging effects result in an increase of the internal resistance and can be detected through the impedance monitoring of batteries used in Uninterrupted Power Supply (UPS) systems [17].

Cugnet *et al.* have estimated the battery crank-ability using the definition that the battery crank-ability is correlated to the battery resistance. The Battery crank-ability is the battery's ability to start a vehicle [18]. Okoshi *et al.*, in 2006, employed Kalman Filter (KF) to reduce the estimation errors of SOH based on the AC and DC resistances of lead-acid batteries [19]. In 2009, Moo *et al.* enhanced the Coulomb-counting technique to better estimate the SOC and SOH of lithium-ion batteries [20]. In the same year, Barlak and Özkaznaç used a parametric approach, which is based on the generic electric circuit model of the battery, for the SOH determination [21]. The battery parameters are identified by an algorithm based on the Extended KF (EKF).

In 2004, Hariprakash *et al.* have used the galvanostatic non-destructive technique to monitor the SOH of lead-acid batteries [22]. To achieve this goal, they have analyzed the Ohmic resistance, the charge transfer resistance, and the interfacial capacitance of the battery.

In 1999, Salkind *et al.* [23], and in 2002, Singh and Reisner [24] determined the SOH of lead-acid batteries using fuzzy logic. Then, in 2004, Singh *et al.* applied this method to a 125Ah-12V VRLA battery [25]. In most of these papers, the SOH has been determined using the AC and DC impedance of the battery; hence, the battery must be examine for different frequencies.

Bhangu *et al.* have used Kalman filter to estimate the SOC and employed extended Kalman filter to estimate the SOH of lead-acid batteries. The dynamic model of each cell is composed of two capacitors (bulk and surface) and three resistors (terminal, surface, and end) [26]. In 2009, Gould *et al.* used the same technique but with an adaptive battery model based on the Randles' lead-acid model [27]. Zhang *et al.* employed unscented Kalman filter and a proposed equivalent circuit model to estimate the SOC and SOH [28].

Coleman *et al.* proposed a two-pulsed test to determine the SOC and SOH of VRLA batteries. The first pulse stabilizes the battery relative to its previous history and the second pulse establishes the parameters, which are related to the voltage drop after each pulse of the current discharge [29].

Sun *et al.* proposed a health auxiliary diagnosis method based on sample entropy for lead-acid batteries. In this method, the SOH is estimated at the end of each discharging cycle by measuring the battery voltage and current [30].

Haifeng *et al.* proposed power-reflecting SOH definition and used that to predict the SOH based on parameter system identification [31]. The proposed method were simulated and tested for Hybrid Electric Vehicles (HEVs).

Zheng *et al.* have proposed an algorithm aiming to maximize the battery efficiency for the computer-assisted health-care systems with multiple batteries. Based on an accurate analytical battery model, the concept of weighted battery fatigue degree is introduced and the novel battery-scheduling algorithm is called the Predicted Weighted Fatigue Degree Least First (PWFDLF) is developed [32].

Khare *et al.* proposed an on-line method to estimate the SOH of HEVs from various slopes of battery parameters such as the internal resistance, the terminal voltage, and the specific gravity [33]. They showed that the regression model, when employed on the discharge profile of automobile batteries, indicates correlation between these battery parameters.

Saha *et al.* used Relevance Vector Machines (RVMs) and Particle Filters (PFs) to estimate the RUL of batteries based on the electrochemical processes in the form of equivalent electric circuit parameters combined with the statistical models of state transitions, aging processes, and measurement fidelity in a formal framework [34]. Kim has employed a dual-sliding-mode observer to estimate the SOH of Lithium batteries. The observer consists of a fast-paced time-varying observer, which estimates parameters such as the state of charge and terminal voltage, and polarization, and a slow-paced time-varying observer, which estimates the SOH in terms of the capacity fade and resistance deterioration [35].

To summarize, the proposed methods for estimating the SOH of batteries in literatures can be categorized into two groups:

- Estimating the SOH in laboratories using different parameters such as temperature in a wide range
- Estimating the SOH based on the AC and DC impedances and the AC conductance

In this paper, the SOC and SOH of VRLA batteries are determined using the electric model of the battery, which is based on the electrochemical properties and variations of the current and voltage during the charge and discharge processes. The electric model is identified using the Radial Basis Function (RBF) Neural Network (NN). Then, using the SOC as one of the state space variables and employing the Extended Kalman Filter (EKF), the SOC is estimated. Next, based on the relation between the SOC and the battery open-circuit voltage and according to the observations made in different

experiments performed on VRLA batteries with various ages, it will be shown that the SOH can be determined using the slope of the *Q-VOC* curve, where *Q* is the stored charge in the battery and *VOC* is the battery open-circuit voltage. Then, using the battery open-circuit voltage (i.e. the battery terminal voltage when no current is passing though the terminals) and the estimated SOC, the slope of this curve will be estimated using the Least Square (LS) method. Finally, the SOH will be defined by designing an appropriate fuzzy system, whose input is the estimated slope of the *Q-VOC* curve and its output is the projected SOH. All these steps will be performed for the charging as well as discharging processes. One of the major advantageous of the proposed method is that it is independent of the battery Ah and/or the battery type (e.g. lead-acid, lithium-ion, etc.). In order to show effectiveness of the proposed method, the estimated SOH of two batteries with the unknown SOH (50% and 80%) are given. Moreover, the employed batteries in this paper are from two different manufacturers. In addition, the pulse charging method, in which a series of voltage or current pulses is fed to the battery, is employed in this paper. In this charging method, the DC pulses have a strictly controlled rise time, pulse width, pulse repetition rate (frequency) and amplitude. This technology is said to work with batteries of any size, voltage, capacity or chemistry. Moreover, in this charging technique, high instantaneous voltages can be applied without overheating the battery. This can break down the lead-sulfate crystals in lead-acid batteries, thus greatly extending the battery service life.

The proposed method has been implemented in room temperature. For extending the proposed method for different ambient temperatures, some suggestions are given at the end of the paper.

The rest of this paper is organized as follows. Section 2 describes estimation of the SOC using EKF and a model based on the RBFNN. Section 3 shows how the SOH can be estimated using the slope of the *Q-VOC* curve. Section 4 describes design of the fuzzy system for the SOH estimation. Section 5 gives experimental results and discussions. Section 6 concludes the paper.

2. SOC ESTIMATION USING EKF

The SOC can be defined as the ratio between the saved energy in a battery and the whole energy that could be saved in it [36]

$$SOC(t) = SOC(t_0) \int_{t_0}^{t} \frac{\eta I(\tau)}{Q_0} d\tau \tag{1}$$

where $SOC(t_0)$ is the initial SOC, Q_0 is the nominal capacity, I(t) is the instantaneous current (positive for charge and negative for discharge), and η is the Columbic efficiency ($\eta \le 1$ for charge and $\eta = 1$ for discharge). In order to employ the EKF, it is necessary to discretize the model in (1). Assuming that the sampling rate Δt is small enough and substituting the integral with the Euler approximation, (1) can be written as

$$SOC(k+1) = SOC(k) + \frac{\eta \, \Delta t}{Q_0} I(k) \tag{2}$$

In this paper, the SOC is considered as one of the state variables of the battery and is directly estimated using EKF. Since EKF needs an appropriate model of the system, RBF Neural Network (RBFNN) is employed for the state-space modeling of the battery [37]. Fig.1 shows the structure of an RBFNN, where the inputs are the battery terminal voltage, the calculated SOC using the Ampere-hour counting technique, and the battery terminal current all at the sampling time *k*. The NN finds an approximation of the battery terminal voltage at the sampling time *k*+1. The activation functions of neurons in the hidden layer are Gaussian functions [38]:

$$\varphi_i(\mathbf{r}_k) = G\left(\left\|\mathbf{r}_k - \mathbf{t}_i\right\|\right) = \exp\left(-\frac{\left\|\mathbf{r}_k - \mathbf{t}_i\right\|^2}{\sigma_i^2}\right), \quad i = 1, \ldots, M \tag{3}$$

where $\mathbf{r}_k = [V_k \; I_k \; SOC_k]^T$ is the input vector applied to the network at the sampling time *k*, $\mathbf{t}_i$ and σ_i are the center and the standard deviation of the Gaussian function, respectively, and *M* is the number of neurons in the hidden layer. In fact, the output of this NN (i.e. the battery terminal voltage at the sampling time $(k+1)$ is the sum of the weighted Gaussian functions as

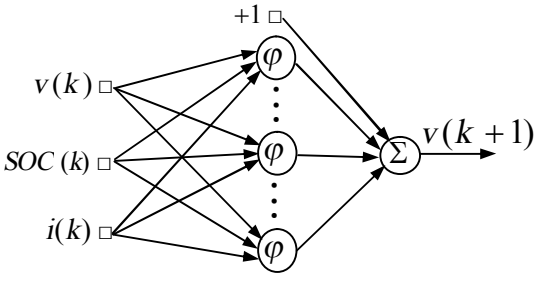

Fig. 1. Structure of the RBF neural network for modeling.

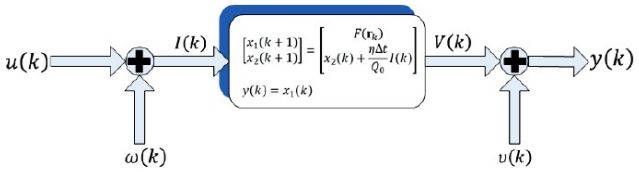

Fig. 2. Construction of EKF for state estimation of battery.

$$V_{k+1} = F(\mathbf{r}_k) = w_0 + \sum_{i=1}^{M} w_i \varphi_i(\mathbf{r}_k) \tag{4}$$

where w_i (i=1, …, M) is the synaptic weight connecting the i^{th} neuron in the hidden layer to the output layer and w_0 is the bias weight for the linear output neuron. The free parameters of this network are $\mathbf{t}_i$, σ_i, w_i, and w_0. These parameters can be defined during the training phase of the network using algorithms such as error back-propagation and least-mean-square error [38].

Considering the battery terminal voltage and SOC at the sampling time k as the first and the second state variables, respectively, the state vector of the system is defined as

$$\mathbf{x}_k := \begin{bmatrix} x_1(k) \\ x_2(k) \end{bmatrix} = \begin{bmatrix} V(k) \\ SOC(k) \end{bmatrix}. \tag{5}$$

Using the above definition, the state-space model can be described as:

$$\begin{cases} \begin{bmatrix} x_1(k+1) \\ x_2(k+1) \end{bmatrix} = \begin{bmatrix} F(\mathbf{r}_k) \\ x_2(k) + \Delta t \left(\dfrac{\eta}{Q_0} I(k) \right) \end{bmatrix} \\ y(k) = V(k) = x_1(k) \end{cases} \tag{6}$$

where $F(\mathbf{r}_k)$ is the nonlinear function in (4).

According to the general approximation theory, the RBFNN can approximate any continuous nonlinear function (such as $F(\mathbf{r}_k)$) with desired accuracy [38].

Since the state-space model of the battery is nonlinear, EKF is used here for the state estimation (Fig. 2). The nonlinear state transition matrix is

$$\mathbf{f}(\mathbf{x}_k, \mathbf{u}_k) = \begin{bmatrix} F(\mathbf{r}_k) \\ x_2(k) + \Delta t \left(\dfrac{\eta}{Q_0} I(k) \right) \end{bmatrix}. \tag{7}$$

By linearizing (7) around the operating point (i.e. the estimated values of the state variables $\hat{\mathbf{x}}_k$), the transient matrix $\mathbf{A}$, the input matrix $\mathbf{B}$, and the measurement vector $\mathbf{C}$ can be obtained as

$$\begin{aligned} \mathbf{A}(k) &= \frac{\partial \mathbf{f}(\mathbf{x}_k, \mathbf{u}_k)}{\partial \mathbf{x}_k} = \begin{bmatrix} \dfrac{\partial F(\mathbf{r}_k)}{\partial \mathbf{x}_k} \\ 0 \quad 1 \end{bmatrix} \\ \mathbf{B}(k) &= \frac{\partial \mathbf{f}(\mathbf{x}_k, \mathbf{u}_k)}{\partial \mathbf{u}_k} = \begin{bmatrix} \dfrac{\partial F(\mathbf{r}_k)}{\partial \mathbf{u}_k} \\ \dfrac{\eta . \Delta t}{Q_0} \end{bmatrix} \\ \mathbf{C} &= \begin{bmatrix} 1 & 0 \end{bmatrix}. \end{aligned} \tag{8}$$

Hence, the linearized process and the measurement equations are

$$\begin{aligned} \mathbf{x}(k+1) &= \mathbf{A}\mathbf{x}(k) + \mathbf{B}\mathbf{u}(k) + \mathbf{B}_1 \omega(k) \\ \mathbf{y}(k) &= \mathbf{C}\mathbf{x}(k) + \upsilon(k) \end{aligned} \tag{9}$$

where $\omega(k)$ is the process noise, and $\upsilon(k)$ is the measurement noise with covariance matrices as

$$\begin{aligned} \mathbf{Q} &:= \mathrm{E}\{\omega(k)\omega^T(k)\} \\ \mathbf{R} &:= \mathrm{E}\{\upsilon(k)\upsilon^T(k)\} \end{aligned} \tag{10}$$

Since there exist only one process noise (i.e. the battery terminal current) and one measurement noise (i.e. the measured battery terminal voltage) matrices $\mathbf{R}$ and $\mathbf{Q}$ reduce to positive scalars.

This fact that the process noise stems only form the input of the system, yields $\mathbf{B}$=$\mathbf{B}_1$ in (9).

During time-update, the covariance matrix for the propagation of the error estimation can be written as [39]

$$\mathbf{M}(k+1) = \mathbf{A}\mathbf{P}(k)\mathbf{A}^T + \mathbf{B}\mathbf{Q}\mathbf{B}^T \tag{11}$$

where $\mathbf{P}(k)$ is the covariance matrix for the state estimation error during the measurement update. At every step, matrix $\mathbf{M}$ is updated using the term $\mathbf{BQB}^T$. Moreover, matrix $\mathbf{B}$ is defined based on the system model and changes in the system updates. Hence, $\mathbf{BQB}^T$, which is semi definite, adaptively changes $\mathbf{M}$.

The covariance for the measurement noise ($\mathbf{R}$) can be calculated using the measured terminal voltage of the battery. For one of the experimental batteries in this paper, this covariance has been calculated as $\mathbf{R}$=0.0073. The covariance for the process noise ($\mathbf{Q}$) has also been set equal to 10. Figs. 3 and 4 show the estimated SOC and the terminal voltage of a VRLA battery with the nominal capacity of 2.5 Ah and terminal voltage of 2 V. As these figures show, the estimation error of the EKF is relatively high. In most applications, the covariance of the measurement noise is set to higher values than calculated for better estimation. Figs. 5 and 6 show the experimental results with $\mathbf{R}$=1. Since the estimated variables are obtained with good accuracy, $\mathbf{R}$=1 and $\mathbf{Q}$=10 will be used throughout the rest of this paper.

Figs. 7 and 8 show the elements of matrices $\mathbf{A}$ and $\mathbf{B}_Q = \mathbf{BQB}^T$, where

$$\mathbf{B}_Q = \mathbf{BQB}^T = \begin{bmatrix} B_{11} \\ B_{21} \end{bmatrix} \mathbf{Q} \begin{bmatrix} B_{11} & B_{21} \end{bmatrix} = \begin{bmatrix} B_{11}^2 & B_{11}B_{21} \\ B_{11}B_{21} & B_{21}^2 \end{bmatrix} = \begin{bmatrix} B_{q11} & B_{q12} \\ B_{q21} & B_{q22} \end{bmatrix}. \tag{12}$$

Based on (8), the matrix elements B_{q11}, B_{q12}, and B_{q22} are very small due to the small value of sampling rate Δt.

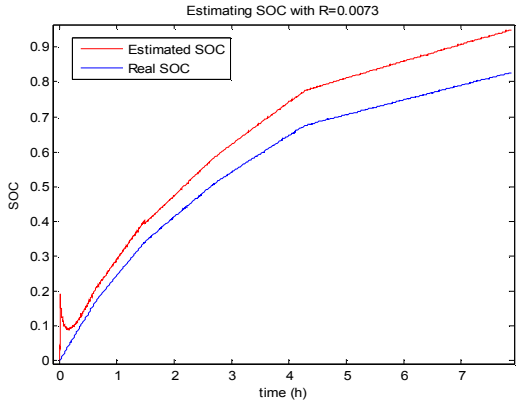

Fig. 3. Estimated SOC of a VRLA battery using EKF with R=0.0073

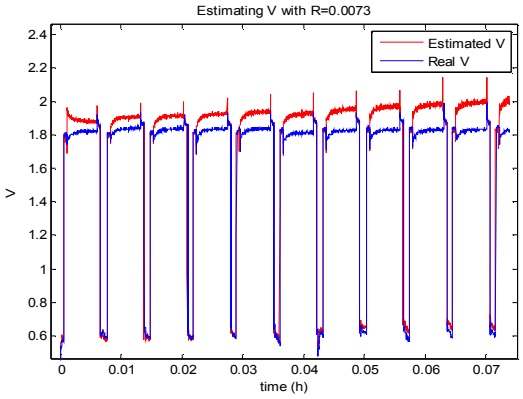

Fig. 4. Estimated terminal voltage of a VRLA battery using EKF with R=0.0073

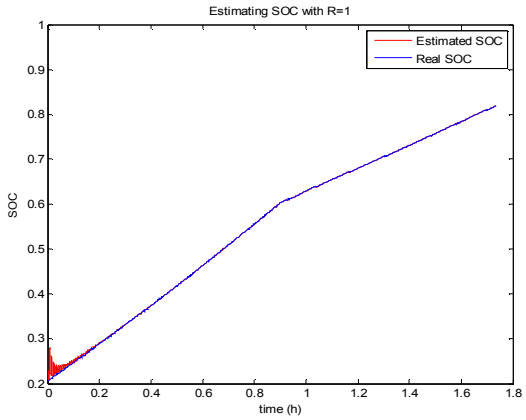

Fig. 5. Same as Fig. 3 but with **R**=1.

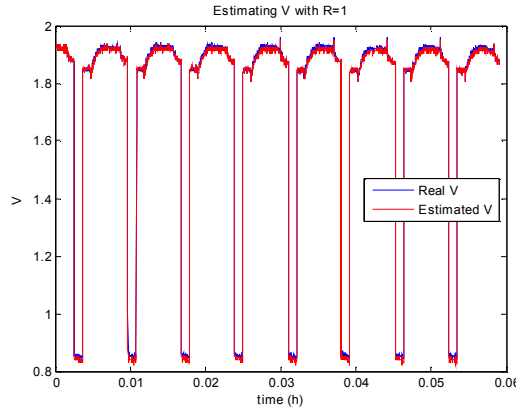

Fig. 6. Same as Fig. 4 but with **R**=1.

3. SOH ESTIMATION

The SOH can be calculated using the following equation [20] and [40]:

$$\text{SOH} = \frac{Q_{max}\,(\text{aged})}{Q_{max}\,(\text{new})} \tag{13}$$

where Q_{max}(aged) and Q_{max}(new) are the theoretical maximum amount of charge that can be drawn from the aged and new battery, respectively.

Equation (13) must be used off-line. That is, the battery must be discharged completely, and then charged and Q_{max} is estimated with any known method such as the Ampere-hour technique. In this paper, the SOH of four batteries (i.e. batteries with the SOH equal to 100%, 72%, 64%, and 46%) are determined using (13) and the Ampere-hour technique. The data of three batteries (100%, 64%, and 46% SOH) are used to construct the structure of the proposed method based. Then, the data of the fourth battery (SOH=72%) is used for testing the proposed method.

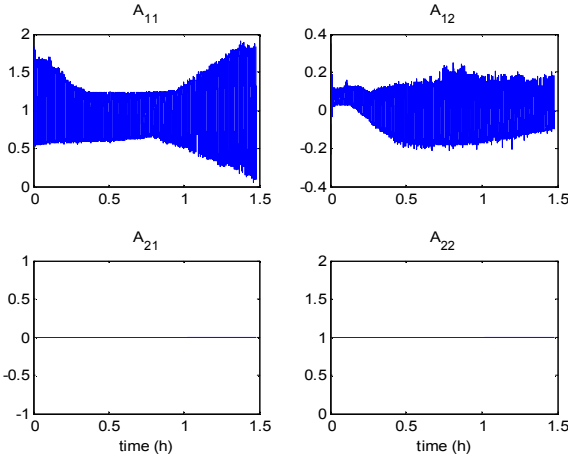

Fig. 7. Elements of matrix **A.**

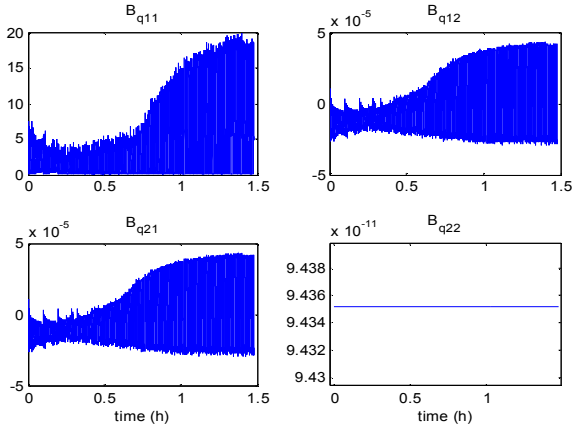

Fig. 8. Elements of matrix $\mathbf{B}_Q$.

Therefore, data collected from three VRLA batteries with the SOH equal to 100%, 64%, and 46% are used for training three RBFNNs. That is, three RBFNNs are trained offline, one for every battery, to estimate the corresponding SOC using EKF and the model defined in (6). Then, the SOH is estimated online based on the Recursive Least Square (RLS) and the fuzzy logic using the SOC and the battery open-circuit voltage. In the followings, we show the relationship between the SOC and the battery open-circuit voltage.

Fig. 9 shows the dynamic model of VRLA batteries [41]. This model has been widely used for simulation of VRLA batteries subject to constant, pulse, and variety of currents. In this model, R_i is the lumped resistance due to cell interconnections, $C_{surface}$ represents the charge separation at the common surface of the electrode/electrolyte, R_t is the impedance characteristic of $C_{surface}$ representing the charge transfer polarization, and C_{bulk} shows the storage capacity of the battery. Since $C_{surface}$ is small, it discharges into R_t when the battery is in rest. Hence, when the circuit is in the steady state, the open-circuit voltage (VOC) of the battery is the voltage across C_{bulk}. Moreover, it can be shown that the VOC of a VRLA battery has a linear relationship with its SOC as [42]

$$VOC(t) = a_1 \mathrm{SOC}(t) + a_0 \tag{14}$$

Capacitor C_{bulk} in Fig. 9 represents the storage capacity of a battery and therefore, is directly proportional to the age of the battery.

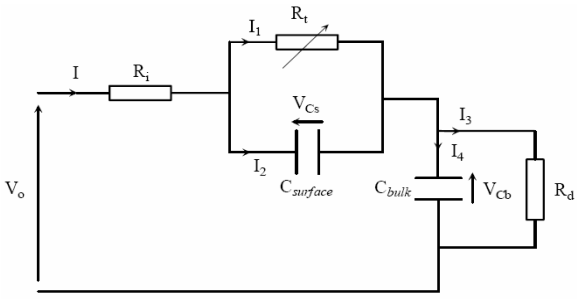

Fig. 9. Dynamic model of VRLA batteries.

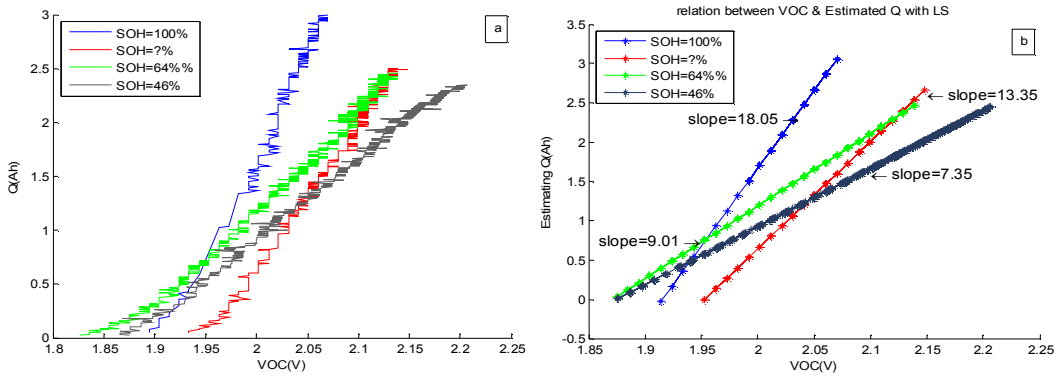

Fig. 10. The graph of Q vs. VOC of 4 batteries with different SOH during charging process (a) experimental result, (b) estimation of straight line using LS method.

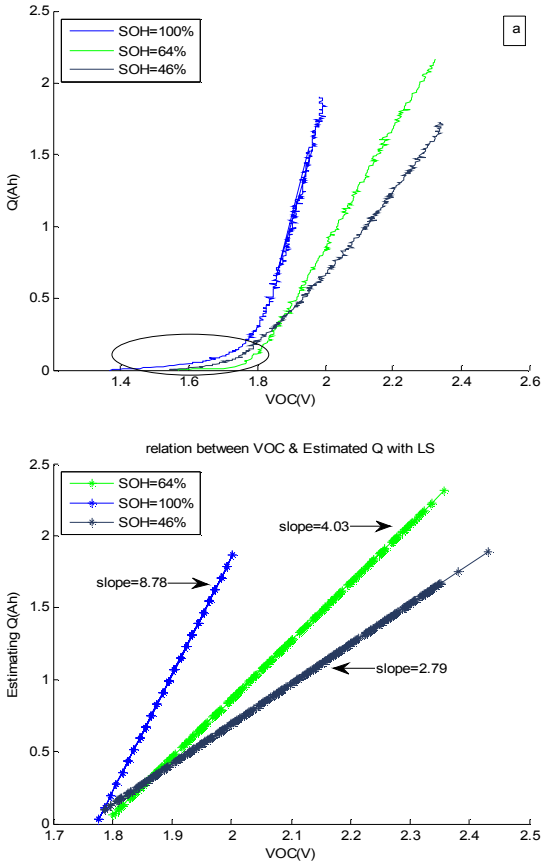

Fig. 11. Same as in Fig. 9 but for discharging process.

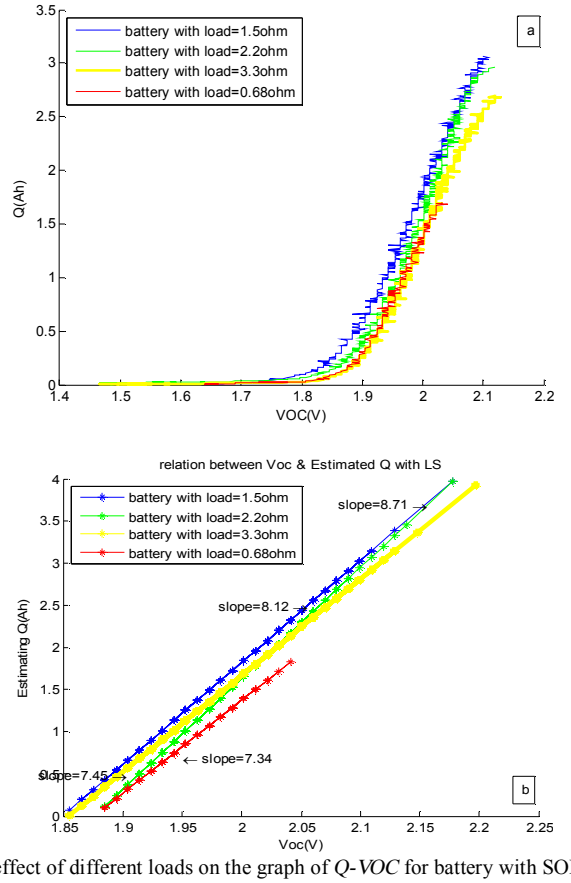

Fig. 12. The effect of different loads on the graph of *Q-VOC* for battery with SOH=100%.

Table 1.Slopes of *Q-VOC* graph of three VRLA batteries with different SOH

SOH	Slope of *Q-VOC* graph	
	for charging	for discharging
100%	18.05	8.78
64%	12.01	4.03
46%	7.36	2.79

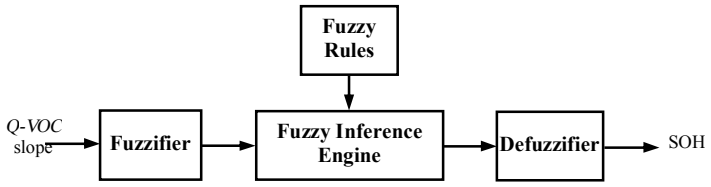

Fig. 13. Structure of the fuzzy system for SOH estimation.

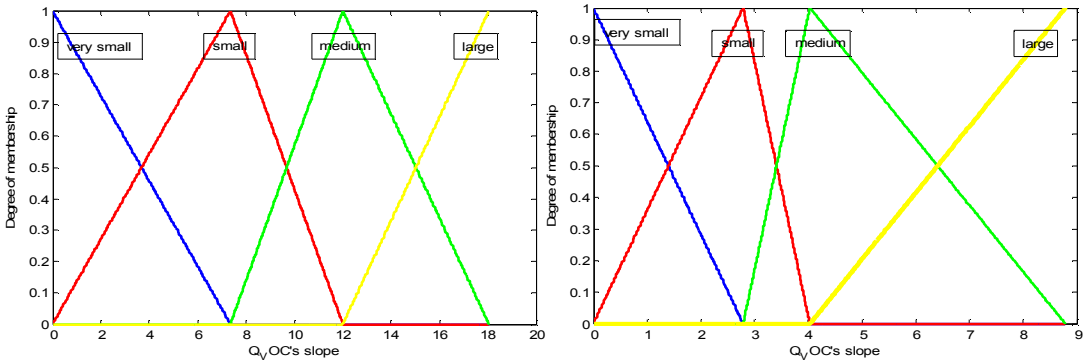

Fig. 14. Fuzzy membership functions for input variable of fuzzy system for (a) charging process and (b) discharging process.

Consider a new battery and a used battery and assume that the same amount of charge Q is loaded in them. Since the storage capacity of the used battery is less than that of a new battery hence, based on $Q=CV$ it can be concluded that the open-circuit voltage of the aged battery must be higher than that of the new battery because the capacitance of the aged battery is lower than that of the new battery. This fact can be observed from the experimental results shown in Fig. 10. Fig. 10(a) shows the relationship between the open-circuit voltage and the power stored in four batteries with different ages during the charging processes, respectively. Fig. 10(b) shows the estimated slope of the graphs *Q-VOC* in Fig. 10(a) using the Least-Square (LS) method. Fig. 11(a) and (b) show similar graphs as in Fig. 10 but for discharging processes. As Figs. 10 and 11 show, the open-circuit voltage of VRLA batteries has almost a linear relationship with its SOC, except for the lower part of these graphs, where the battery does not contain enough charge cannot be used as a power source. Moreover, it is recommended by manufacturers that lead-acid batteries should not enter into this region due to over discharge problems of them.

The stored power Q (i.e. the SOC) is estimated using the EKF and NN (see Section 2). Moreover, the SOH of these four batteries are determined using (13). The data from three of these batteries with SOH=100% (blue), SOH=64% (green) and SOH=46% (black), are used off-line for constructing a fuzzy system. Then, the SOH of the fourth battery with SOH=72% (red) is estimated on-line using this fuzzy system.

Since the SOH is estimated based on the slope of the *Q-VOC* graph in this paper, the effect of load variations on this graph must be checked first. Fig. 12 shows the effect of four different loads on the *Q-VOC* graph for the new battery (i.e. the battery with SOH=100%). As this figure shows, the slope of *Q-VOC* graph is almost constant for different loads, yielding a slope almost independent of the working condition of the battery for estimation of the SOH. Similar graphs have been obtained for other batteries with different SOHs.

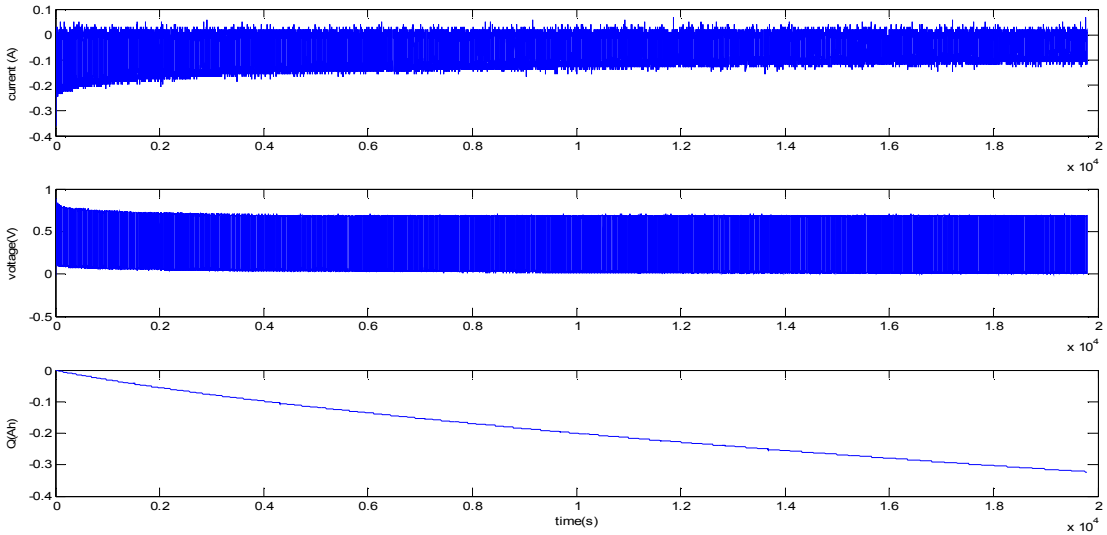

Fig. 16. Voltage, current, and delivered energy of a VRLA battery with SOH=0.46%

Table 2. Fuzzy rules for estimating SOH

	RULE
1	**If** slope is very small, **then** *SOH* is 0%
2	**If** slope is small, **then** *SOH* is 46%
3	**If** slope is medium, **then** *SOH* is 64%
4	**If** slope is large, **then** *SOH* is 100%

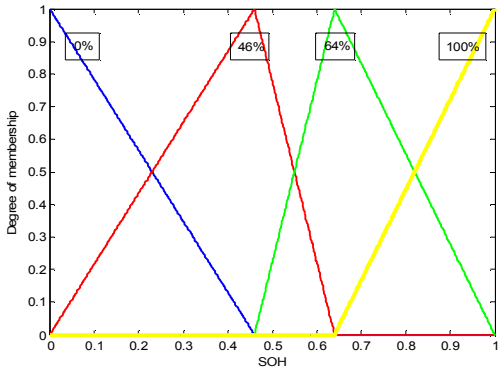

Fig. 15. Fuzzy membership functions for output variable of fuzzy system for charging and discharging processes

.

4. CONSTRUCTING FUZZY SYSTEM FOR SOH ESTIMATION

Table 1 summarizes the slope of graphs in Figs. 10 and 11. It should be noted that the data form three batteries (i.e. batteries with SOH equal to 100%, 64% and 46%) are used to construct the fuzzy system. The SOH of the 4th battery (SOH=72%) is used for testing the proposed method.

The input to the fuzzy system is the slope of the *Q-VOC* graph and the output is the estimated SOH. The structure of the fuzzy system is shown in Fig. 13 [43]. The fuzzy rules are given in Table 2. These rules are formed based on the data in Table 1. The first rule is added artificially in order to obtain a continuous output from the fuzzy system. The output of the fuzzy system is in the range of [0 1]. The fuzzy membership functions for the linguistic variables in Table 2 are shown in Figs. 14 and 15. The center of these membership functions are the actual slope of the data given in Table 1. The fuzzifier is of the singleton type and the defuzzifier is of the center-of-average type [43]. It should be noted that since the slope of the *Q-VOC* graph is different for the charging and discharging processes, two fuzzy systems are designed for each processes.

In construction of the fuzzy system, the SOH=46% is considered as a battery with almost no remaining life time. At this SOH, the battery's characteristics have deteriorated so drastically that the battery cannot be used as a power source anymore. This fact can be observed from Fig. 16, where the voltage of this battery is less than 0.7V during discharging process and the total

delivered energy by this battery is less than 0.35 Ah.

All the aforementioned procedures for constructing the proposed SOH estimator are performed off-line. The procedure for the on-line use of this estimator will be explained in the next section.

5. EXPERIMENTAL SETUP AND RESULTS

In Section 2, it was explained how the SOC of VRLA batteries was estimated using EKF and NNs. Then, in Sections 3 and 4, details of a fuzzy system for estimating the SOH, `using the slope of the *Q-VOC* graph, was explained. These steps were performed separately and off-line using the stored data acquired form three batteries with different SOHs. In this section, it will be explained how the SOC and SOH of VRLA batteries can be estimated on-line and in real time using the constructed systems in previous sections.

During each sampling time, the SOC will be estimated using the EKF and the NN model of the VRLA battery. Then, using the estimated SOC and Q_0, the battery power (Q) will be calculated. Next, using the measured open-circuit voltage of the battery and Q, the slope of the *Q-VOC* graph will be defined in real-time. This varying slope will be applied as input to the fuzzy system. The fuzzy system will estimated the SOH of the testing battery based on the linguistic rules of three batteries stored in it. The slope of the *Q-VOC* graph converges in about 120 minutes or less. Hence, in less than 120 minutes the SOH of a battery with unknown SOH will be estimated. In order to measure the open-circuit voltage, while the battery is connected to the circuit, the pulse (or reflex) charging method is employed in this paper (see Fig. 17). Pulse charging method prevents battery deterioration by stimulating the electrodes of the battery and thereby making its life time longer. In other words, by intermittently using pulse currents during the battery charging or discharging, the lead-sulfate crystals in lead-acid batteries will break down, thus greatly extending the battery service life. In this method, in charging mode, the battery is in rest for t_0 seconds, and then it is charged by I_1 for t_1 seconds, followed by a rest for t_2 seconds and finally, discharged by I_2 for t_3 seconds. In this charging method, the open-circuit voltage of the battery can be measured when the battery is in rest at the end of the charging period. During the discharging process, whenever the battery is at rest (no load current is drawn from the battery) the open-circuit voltage should be measured. In many applications, current is not drawn constantly form the battery and *VOC* can be measure at some instants. Even if loads are connected continuously to the battery, the *VOC* can be measured at the beginning and at the end of the discharging period, which can provide an approximate slope of the *Q-VOC* graph.

Fig. 18 shows the bock diagram of the proposed method. As this figure shows, there are three EKFs in block A for three batteries with the SOH equal to 100%, 64%, and 46%, respectively. In order to obtain a proper model for the EKFs, data from these three VRLA batteries are collected and used to train three NNs off-line. The measured current and open-circuit voltage of the testing battery is applied as inputs to block A. The estimated voltage by the EKFs is compared with the measured voltage. The EKF with the least error is selected as the best estimation for the SOC of the unknown battery. This task is performed based on the sum of squared errors between the estimated and the actual voltage during the first two minutes (three cycles) of the charging/discharging process. In the lower part of the block diagram in Fig. 18, the estimated SOC and the *VOC* is used to predict the slope of the *Q-VOC* graph using Recursive Least-Square (RLS) method [44], which is the input to the fuzzy system. The output of the fuzzy system is a number between zero and one indicating the percentage of the remaining life of the battery. The convergence time of the RLS method for the batteries employed in this paper is between 60 and 90 minutes. One of the advantages of using RLS method to estimate the slope of the *Q-VOC* is that it can be used on-line. That is, unlike the LS method, there is no need to collect all data in advance for $\hat{SOC}$ $\hat{V}$ estimating the slope. Moreover, in RLS method, there is a trade-off between the estimation error and the convergence time; hence, the user can adjust some parameters to achieve better estimation error or faster convergence time [44]. Therefore, for off-line construction of the estimator, the LS method has been used, while for on-line estimation, the RLS method is employed. It should be mentioned that this method may not be used in all different applications. However, there are many applications where constant charging or discharging of the battery exists. For instance, many types of battery-operated equipments such as cellular phones, digital cameras, personal pagers, photoflash equipments, portable communication equipments, portable hand tools and appliances, portable computers, radios, electrical shocks, electric shavers, and batteries store room in telecommunication centers, are examples where constant charging or discharging processes exist.

Experimental tests are carried out on VRLA batteries with 2.5 Ah nominal capacity and 2 V nominal voltage. The *VOC*-SOC graph for this battery, provided by the manufacturer, is practically linear from 10% to 100% of the full capacity (Fig. 19) [45].

Figs. 20 and 21 show the charging and discharging graphs for the new battery with SOH=100%, respectively. In order to have rich data for better training the RBFNNs, the batteries are charged with different duty cycles (Table 3). Figs. 22 and 23 show 300 seconds of graphs in Fig. 20. In order to prevent the NNs from overtraining, only 1500 samples of data in Figs. 20 and 21 are used for battery modeling [38]. The standard deviations of the Gaussian functions in (3) are selected fixed for all neurons in the hidden layer and equal to σ_i=0.7 (i=1,…,M), where M=60. Hence, the free parameters of the NNs are the center of the Gaussian functions ($\mathbf{t}_i$), the synaptic weights w_i (i=1,..,M), and w_0 W_0 . Fig. 24 shows that the NN can provide very good estimation of the battery model. The error performance of one of the NNs is shown in Fig. 25. Altogether, three RBFNNs (i.e. $F_i(\mathbf{r}_k)$, i=1,2,3 in (6)) are trained and used in three EKFs, respectively. The initial values of the state variables of EKFs can be selected to any number between zero (i.e., the empty battery) and one (i.e. the full battery).

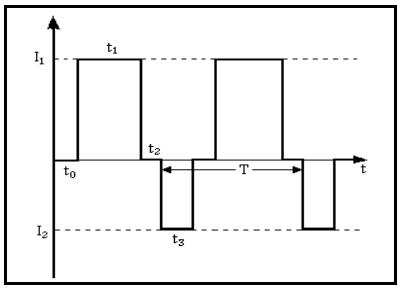

Fig. 17. Current waveform for pulse charging method.

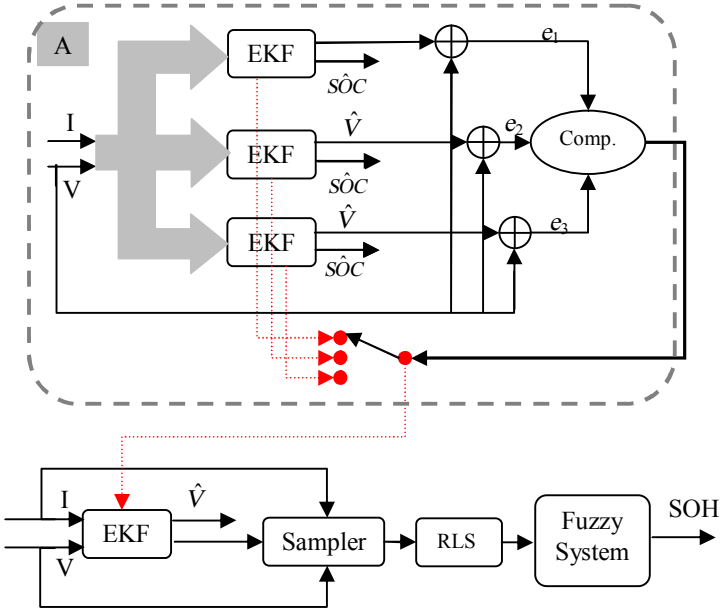

Fig. 18. Block diagram of the proposed method.

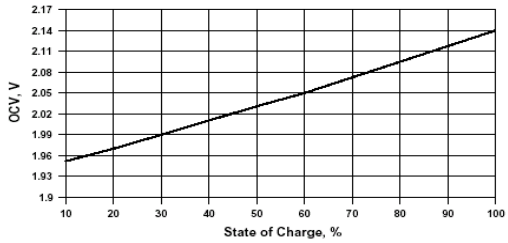

Fig. 19. Graph of open-circuit voltage vs. SOC for VRLA batteries used in this paper (Shenzhen Co. [45]).

Table 3. Different duty cycles for PWM during charging process.

Duty-Cycle	Q_{min} (Ah)	Q_{Max} (Ah)
70%	0	1
55%	1	1.5
40%	1.5	2
25%	2	2.5
11%	2.5	3

In order to show the effectiveness of the EKFs in estimating the actual states of the batteries, the following cases are considered:

1- Charging processes:

- the initial value of the EKFs states are set to zero and the battery is completely discharged (Fig. 26 (a)).
- the initial value of the EKFs states are set to zero; however, the battery contains 26% of its full charge (Fig. 26 (b)).

2- Discharging processes:

- the battery contains 80% of its full charge and the initial values of the EKFs states are set to the same value (Fig. 27 (a)).
- the battery contains 80% of its full charge; however the initial values of the EKFs states are set to one (Fig. 27 (b)).

The actual SOCs in Figs. 26 and 27 are determined using the Ampere-hour counting technique. As these figures show, the estimated SOC quickly converges to the actual SOC, both for the charging as well as the discharging processes. The convergence time is between 5 and 10 minutes, depending on the initializations.

Next, the simultaneous and on-line estimation of the SOC and the SOH of three VRLA batteries with SOH equal to 100%, 64%, and 46% are performed (Fig. 28, 29). As this figure shows, the maximum estimation error for the SOHs is just 3% for the new battery (SOH = 100%) during the charging process. Moreover, the convergence time of is between 60 and 90 minutes.

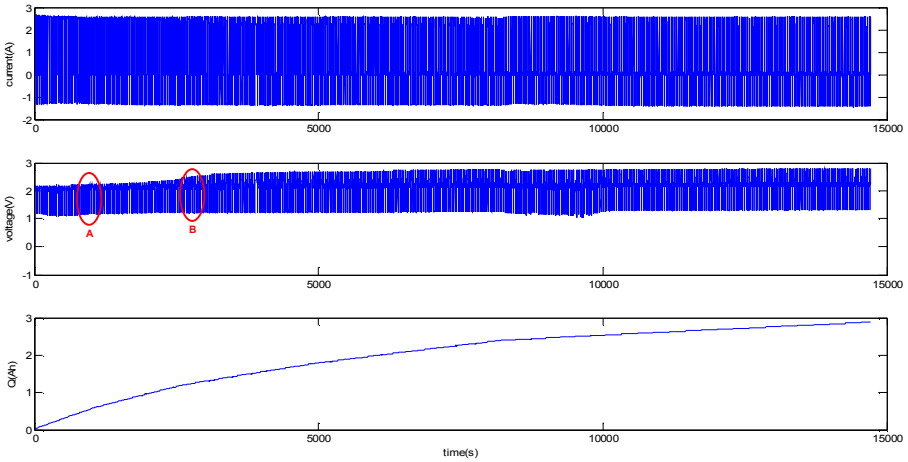

Fig. 20. Current, voltage, and power stored in a new VRLA battery during charging process using different duty cycles given in Table 3.

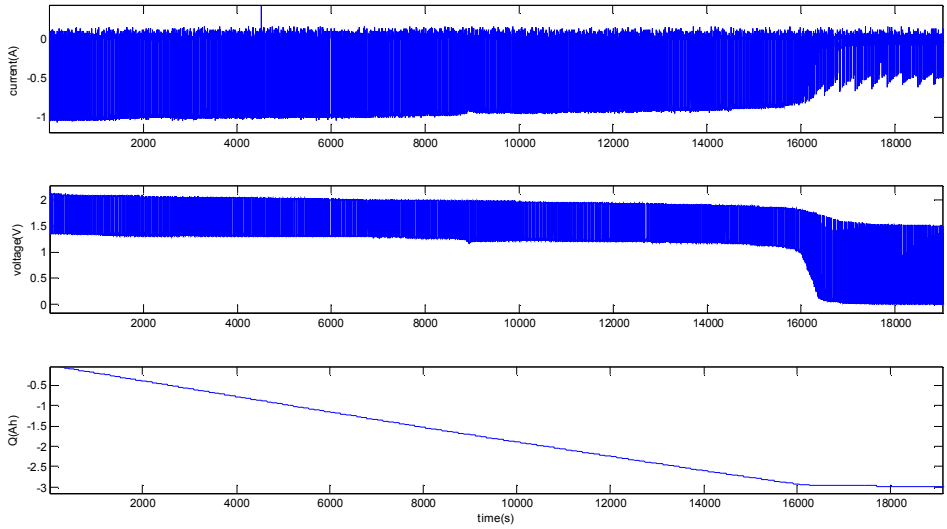

Fig. 21. Same as Fig. 19 but for discharging process.

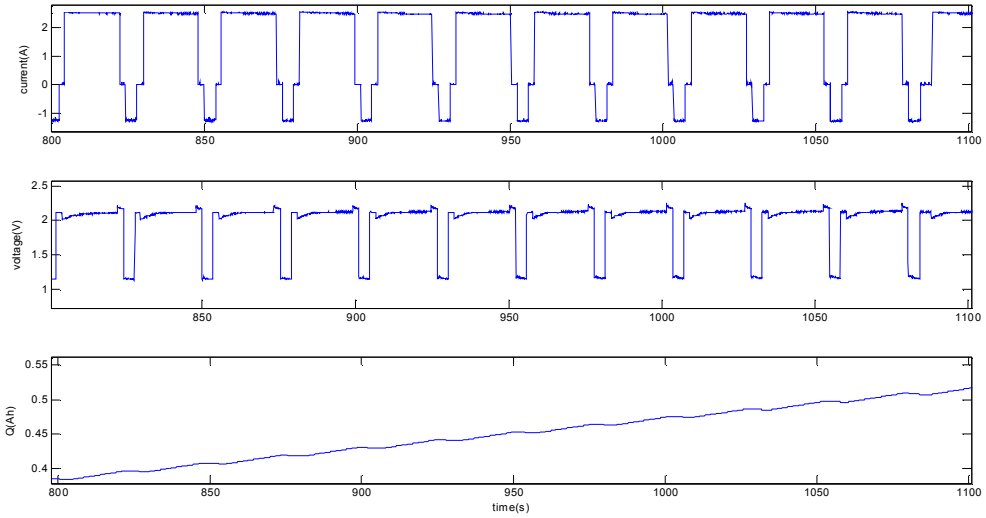

Fig. 22. 300 seconds of plots in Fig. 20 (area shown with circle A).

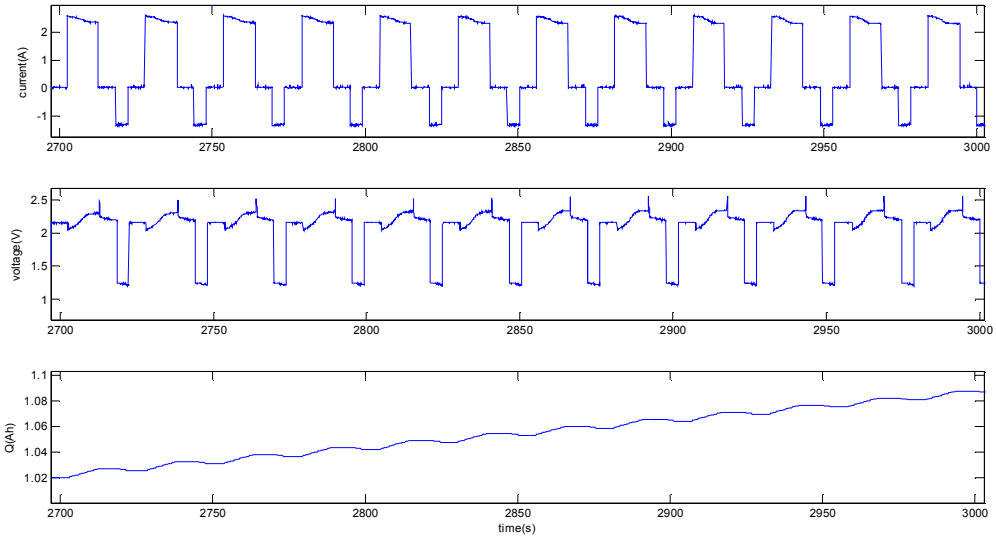

Fig. 23. 300 seconds of plots in Fig. 20 (area shown with circle B)

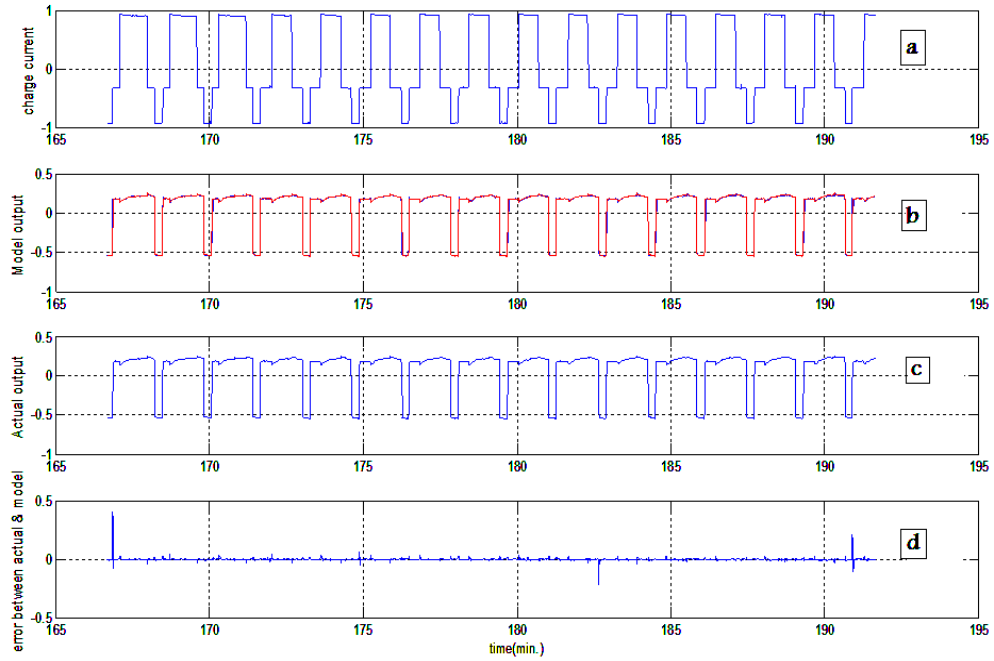

Fig. 24. (a) Battery current (NN input), (b) actual (red) and estimated (blue) battery voltage, (c) actual (measured) battery voltage, (d) estimation error.

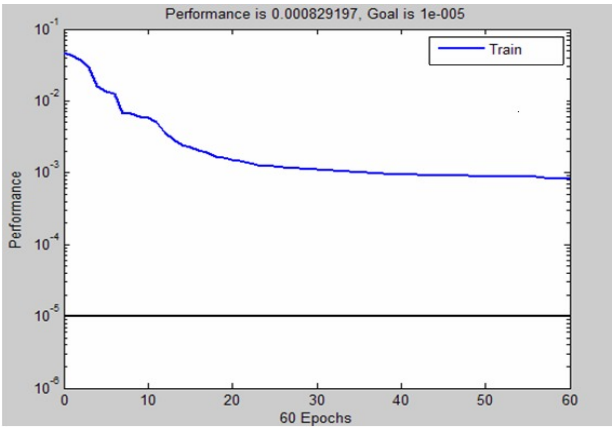

Fig. 25. Sum of squared errors for one of the NNs.

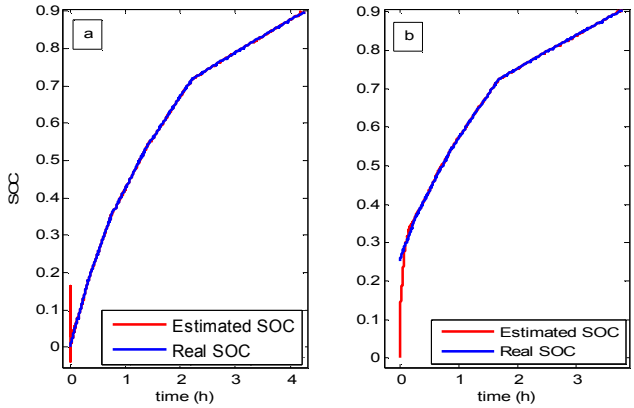

Fig. 26. SOC estimation during charging process(a) initialization is equal to the actual SOC, (b) different initialization.

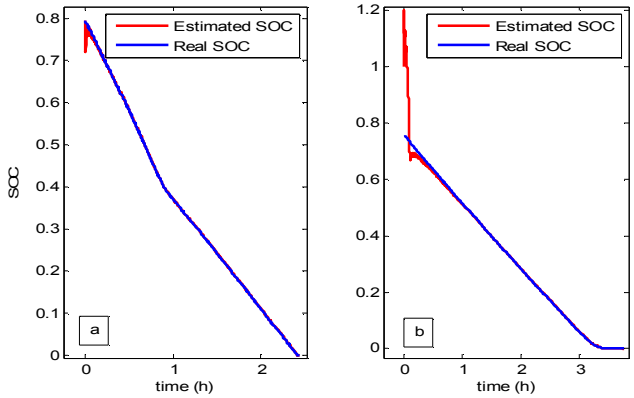

Fig. 27. Same as Fig. 26 but for discharging processes.

It should be noted that two estimators (shown in Fig. 18) are designed in this paper: one time for the charging processes and another time for the discharging processes, each with three EKFs, three NNs, and one fuzzy system.

Next, the simultaneous and on-line estimation of the SOC and the SOH of three VRLA batteries with SOH equal to 100%, 64%, and 46% are performed (Fig. 28 and 29). As this figure shows, the maximum estimation error for the SOHs is just 3% for the new battery (SOH = 100%) during the charging process. Moreover, the convergence time of is between 60 and 90 minutes. Table 4 summarizes the actual and the estimated SOHs for the charging and discharging processes of three VRLA batteries used in constructing the proposed SOH estimator in this paper.

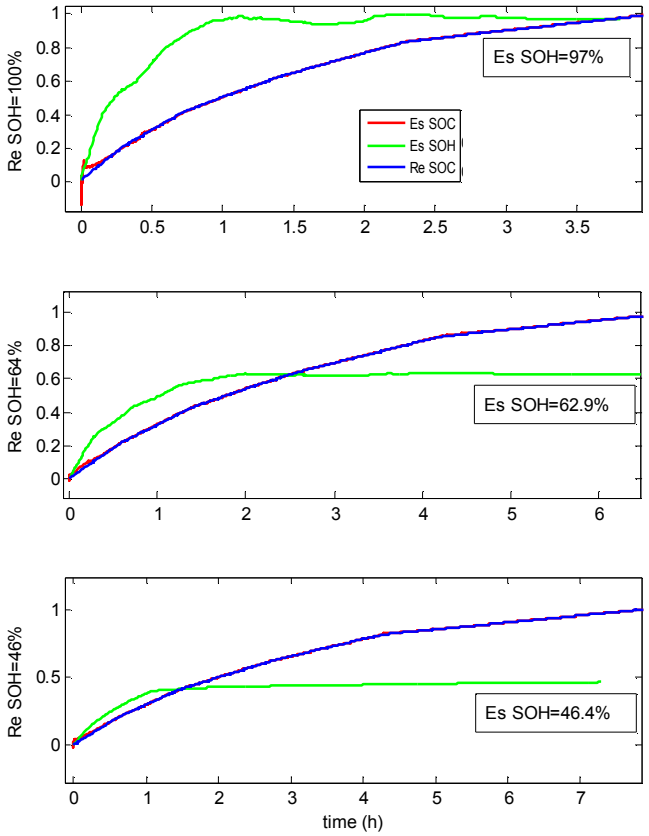

Fig. 28. Simultaneous estimation of SOC and SOH during charging for three batteries with SOH equal to 100% (top), 64% (middle), and 46% (bottom).

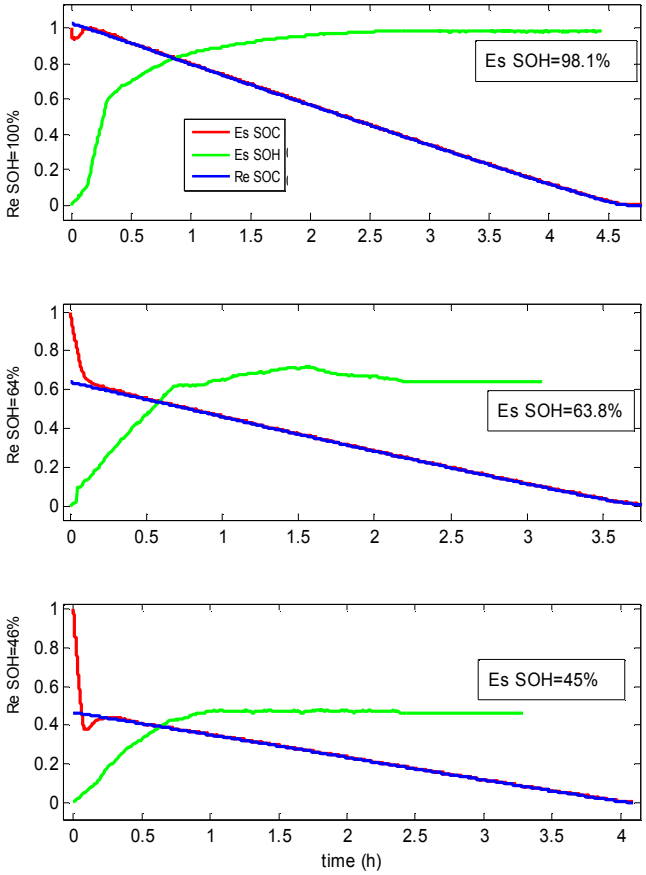

Fig. 29. Same as Fig. 28, but during discharging .

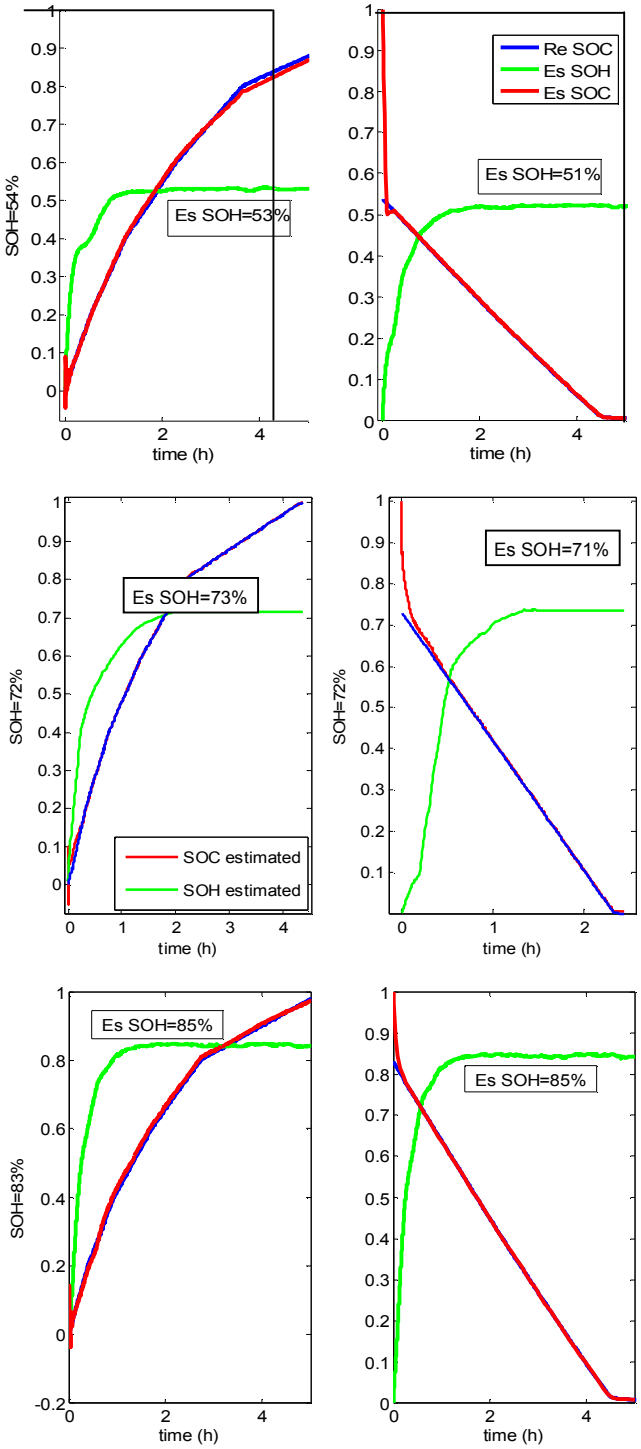

Fig. 30. Estimation of SOC and SOH of three test battery during charging (left) and discharging (right).

Table 4. Summary of estimated SOHs for three known batteries.

Battery	Actual SOH	Estimated SOH during Charging	Estimated SOH during Discharging
1	100%	97%	98.1%
3	64%	63%	63.8%
4	46%	46.4%	45%

Table 5. Summary of estimated SOHs for three unknown batteries.

Battery	Actual SOH	Estimated SOH during Charging	Estimated SOH during Discharging
1	54%	53%	51%
2	72%	71%	73%
3	83%	85%	85%

Next, the proposed method is tested for three batteries with unknown SOH, whose data has not been used for constructing the estimator shown in Fig. 18. In other words, no data from these batteries have been used in training the NNs and in building the fuzzy system. It should be noted that the SOC and the SOH estimations are on-line and in real time. For the sake of comparison, the actual SOH of this battery is determined off-line using (13) and are equal to 54%, 72%, and 85%, respectively. Fig. 30 shows the experimental results. The values of the estimated SOHs for these three batteries are given in Table 5. The convergence time is less than two hours for the charging and discharging processes. As these figure show, the proposed method is able to estimate the SOH of the unknown battery with relatively good accuracy.

6. CONCLUSION AND DISCUSSIONS

A new method for the on-line estimation of the State of Health (SOH) of VRLA batteries was presented in this paper. The proposed method is based on the State of Charge (SOC) of the battery. The SOC was estimated based on the Extended Kalman Filter (EKF) and a neural network model of the battery. To this end, data from three batteries were collected and used off-line to obtain a proper model for three EKFs, respectively. The proposed method identifies the fittest EKF to the testing battery in less than two minutes (three cycles) during the charging or discharging processes. Then, the SOH was estimated on-line based on the relationship between the SOC and the battery open-circuit voltage using the fuzzy logic and the recursive least square method. The experimental results showed good estimation of the SOH of VRLA batteries. The main advantage of the proposed method, besides its good accuracy, is that it can be used on-line and there is no need to disconnect the battery form the circuit.

A few issues about the proposed method need to be discussed here. These issues can give directions to the future works:

- It should be noted that in order to accurately determine the SOH of a battery using the proposed method, the battery must be continually charged or discharged. Hence, the application of the proposed method in cases where an alternator smoothes out large part of the current variations (such as in a car) may not yield accurate results. This is an issue, which is considered for future works of this paper.
- The proposed method was carried out in room temperature. However, some batteries are used in different ambient temperatures. The simplest way to incorporate the battery thermal effect into the proposed method is to create a look-up table composed of different models [46]. In other words, one estimator should be constructed for every range of say 10 ^{o}C of the ambient temperature. This, of course, requires more memory for data storage and processing.

REFERENCES

[1] E. Meissner and G. Richter, "Battery monitoring and electrical energy management precondition for future vehicle electric power systems," *J. Power Sources,* vol. 116, no. 2, pp. 79–98, 2003.

[2] A. Szumanowski and Y. Chang, "Battery management system based on battery nonlinear dynamics modeling," *IEEE Trans. Veh. Technol*, vol.57, no. 3, pp. 1425–1432, May. 2008.

[3] B. P. Divakar, K. W. E. Cheng, H. J. Wu, J. Xu, H. B. Ma, W. Ting, K. Ding, W. F. Choi, B. F. Huang, and C.H. Leung, "Battery management system and control strategy for hybrid and electric vehicle," *Int. Conf. Power Electron. Syst. Appl*., Hong Kong, 2009, pp. 1–5.

[4] B. Pattipati, K. Pattipati, J. P. Christopherson, S.M. Namburu, D.V. Prokhorov, and L. Qiao, "Automotive battery management systems," *IEEE Autotestcon*, Storrs, CT, USA, Sep. 2008, pp. 581–586.

[5] R. Kaiser, "Optimized battery-management system to improve storage lifetime in renewable energy systems," *J. Power Sources,* vol. 168, no. 1, pp. 58–65, 2007.

[6] Y. S. Wong, W. G. Hurley, and W. H. Wölfle, "Charge regimes for valve-regulated lead-acid batteries: Performance overview inclusive of temperature compensation," *J. Power Sources,* vol. 183, pp. 783–791, 2008.

[7] A. Salkind, T. Atwater, P. Singh, S. Nelatury, S. Damodar, C. Fennie Jr, and D. Reisner, "Dynamic characterization of small lead-acid cells," *J. Power Sources,* vol. 96, no. 1, pp. 151–159, 2001.

[8] P. E. Pascoe and A. H. Anbuky, "A VRLA battery simulation model," *Energy Convers. Manag.*, vol. 45, pp. 1015–1041, 2004.

[9] A. Jossen, "Fundamentals of battery dynamics," *J. Power Sources*, vol. 154, no. 2, pp. 530–538, 2006.

[10] I. Damlund, "Analysis and interpretation of AC-measurements on batteries used to assess state-of -health and capacity-condition," *IEEE Telecommun. Energy Conf.*, Hague, Netherlands, 1995, pp. 828–833.

[11] D. C. Cox and R. Perez-Kite, "Battery state of health monitoring combining conductance technology with other measurement parameters for real -time battery performance analysis," *IEEE Telecommun. Energy Conf.*, Phoenix, AZ, USA, 2000, pp. 342–347.

[12] P. E. Pascoe and A. H. Anbuky, "Standby Power System VRLA Battery Reserve Life Estimation Scheme," *IEEE Trans. Energy Convers.*, vol. 20, no. 4, pp. 887–895, Dec. 2005.

[13] C. S. C. Bose and T. Laman, "Battery state of health estimation through coup de fouet: field experience," *IEEE Telecommun. Energy Conf.*, Phoenix, AZ, USA, 2000, pp. 597–601.

[14] P. E. Pascoe and A. H. Anbuky, "The behavior of the coup de fouet of valve-regulated lead–acid batteries," *J. Power Sources*, vol. 111, no. 2, pp. 304–319, 2002.

[15] A. Delaille, M. Perrin, F. Huet and L. Hernout, "Study of the "coup de fouet" of lead-acid cells as a function of their state-of-charge and state-of-health," *J. Power Sources,* vol. 158, no. 2, pp. 1019–1028, 2006.

[16] H. Blanke, O. Bohlen, S. Buller, R.W. De Doncker, B. Fricke, A. Hammouche, D. Linzen, M. Thele, and D.U. Sauer, "Impedance measurements on lead–acid batteries for state-of-charge state-of-health and cranking capability prognosis in electric and hybrid electric vehicles," *J. Power Sources,* vol. 144, no. 2, pp. 418–425, 2005.

[17] M. Kiel, D. U. Sauer, P. Turpin, M. Naveed, and E. Favre, "Validation of single frequency Z measurement for standby battery state of health determination," *30th IEEE Int. Conf. Telecom Energy* (*INTELEC '08*), San Diego, CA, USA, 2008.

[18] M. Cugnet J. Sabatier, S. Laruelle, S. Grugeon, B. Sahut, A. Oustaloup, and J. Tarascon, "On Lead-Acid-Battery Resistance and Cranking-Capability Estimation," *IEEE Trans. Ind. Electron.*, vol. 57, no. 3, pp. 909–917, Mar.2010.

[19] T. Okoshi, K. Yamada, T. Hirasawa and A. Emori, "Battery condition monitoring technologies about lead-acid batteries," *J. Power Sources,* vol. 158, no, 2, pp. 874–878, 2006.

[20] K. S. Ng, C. S. Moo, Y. P. Chen, and Y. C. Hsieh, "Enhanced coulomb counting method for estimating state-of-charge and state-of-health of lithium-ion batteries," *Applied Energy,* vol. 86, pp. 1506–1511, 2009.

[21] C. Barlak and Y. Özkaznaç, "A classification based methodology for estimation of state-of-health of rechargeable batteries," *Int. Conf. Elec. Electron. Eng.* (*ELECON 2009*), Bursa, Turkey, 2009.

[22] B. Hariprakash, S. K. M. Jaikumar, and A. K. Shukla, "On-line monitoring of lead–acid batteries by galvanostatic non-destructive technique," *J. Power Sources,* vol. 137, no. 1, pp. 128–133, 2004.

[23] A. J. Salkind, C. Fennie, P. Singh, T. Atwater, and D.E. Reisner, "Determination of state-of-charge and state-of-health of batteries by fuzzy logic methodology," *J. Power Sources,* vol. 80, no. (1–2), pp. 293–300, 1999.

[24] P. Singh and D. Reisner, "Fuzzy logic-based state-of-health determination of lead acid batteries," *IEEE Telecommun. Energy Conf.*, Villanova, PA, USA, 2002, pp. 583–590.

[25] P. Singh, S. Kaneria, J. Broadhead, X. Wang, and J. Burdick, "Fuzzy logic estimation of SOH of 125Ah VRLA batteries," *IEEE Telecommun. Energy Conf.*, Farmington, CT, USA , 2004, pp. 524–531.

[26] B. S. Bhangu, P. Bentley, D. A. Stone, and C. M. Bingham, "Nonlinear observers for predicting state of-charge and state-of-health of lead-acid batteries for hybrid-electric vehicles," *IEEE Trans. Veh. Technol.*, vol. 54, no. 3, pp. 783-794, 2005.

[27] C. R. Gould, C. M. Bingha, D.A. Stone, and P. Bentley, "New Battery Model and State-of-Health Determination Through Subspace Parameter Estimation and State-Observer Techniques," *IEEE Trans. Veh. Technol.y*, vol. 58, no. 8, pp. 3905–3916, Oct. 2009.

[28] F. Zhang, G. Liu, and L. Fang, "Battery state estimation using Unscented Kalman Filter," *IEEE Robotics and Autom. Int. Conf.*, Kobe, Japan, May. 2009, pp. 1863–1868.

[29] M. Coleman, W.G. Hurley, and C.K. Lee, "An Improved Battery Characterization Method Using a Two-Pulse Load Test," *IEEE Trans. Energy Convers.*, vol. 23, no. 2, pp. 708–713, Jun. 2008. .

[30] Y. H. Sun, H.L. Jo, and J.C. Wu, "Auxiliary diagnosis method for lead–acid battery health based on sample entropy," *Energy Convers. Manag.*, vol. 50, pp. 2250–2256, 2009.

[31] D. Haifeng, W. Xuezhe, and S. Zechang, "A new SOH prediction concept for the power lithium-ion battery used on HEVs," *Veh. Power and Propuls. Conf.*, Sep. 2009, pp. 1649–1653.

[32] N. Zheng, Z. Wu, M. Lin, and L. T. Yang, "Health-Monitoring Systems Based on Electronic Textiles," *IEEE Trans. Inf. Technol. Biomedicine*, vol. 14, no. 2, pp. 350–359, Mar. 2010.

[33] N. Khare, S. Chandra, and R. Govil, "Statistical modeling of SOH of an automotive battery for online indication," *IEEE Telecommun. Energy Conf.*, San Diego, CA, USA, 2008, pp. 1–7.

[34] B. Saha, K. Goebel, S. Poll, and J. Christophersen, "Prognosis methods for battery health monitoring using a Bayesian Framework," *IEEE Trans. Instrum. Meas.*, vol. 58, no. 2, Feb. 2009.

[35] I. S. Kim, "A technique for estimating the state of health of lithium batteries through a dual-sliding-mode observer," *IEEE Trans. Power Electron.*, vol. 25, no. 4, April 2010.

[36] M. Coleman, C.K. Lee, C. Zhu, and W.G. Hurley, "State-of-charge determination from EMF voltage estimation: using impedance, terminal voltage, and current for lead-acid and lithium-ion batteries," *IEEE Trans. Ind. Electron.*, vol. 54, no. 5, pp. 2550–2557, 2007.

[37] M. Charkhgard and M. Farrokhi, "State of charge estimation for lithium-ion batteries using neural networks and EKF," *IEEE Trans. Ind. Electron.*, vol. 57, no. 12, pp. 4178-4187, 2010.

[38] S. Haykin, Neural networks: a comprehensive foundation, 2nd Ed. Prentice Hall, New Jersey, NJ, 1999.

[39] G. F. Franklin, J.D. Powell, and M.L. Workman, Digital Control of Dynamic Systems, 2nd Edition, Addison-Wesley, Reading, MA, 1989.

[40] M. Coleman, C.K Lee, and W.G**.** Hurley, "State of health determination: two pulse load test for a VRLA battery," *IEEE Power Electron. Spec. Conf.*, Jeju, South Korea, 2006, pp. 1–6.

[41] P. Mauracher and E. Karden, "Dynamic modelling of lead/acid batteries using impedance spectroscopy for parameter identification," *J. Power Sources*, vol. 67, pp. 69–84, 1997.

[42] S. Piller, M. Perrin, and A. Jossen, "Methods for state-of-charge determination and their applications," *J. Power Sources,* vol. 96, no. 1, pp. 113–120, 2001.

[43] L. X. Wang, A course in Fuzzy Systems and Control, Prentice Hall, New Jercy, NJ, 1997.

[44] O. Nelles, Nonlinear System Identification, Springer, Berlin, 2001.

[45] Shenzhen Blspower Technology CO. LTD, Datasheet of 2V/2.5Ah Spiral Sealed lead Rechargeable battery, http://www.blsbattery.com.

[46] G. L. Plett, "Extended Kalman filtering for battery management systems of LiPB-based HEV battery packs, part 2: modeling and identification," *J. Power Sources*, vol. 134, pp. 262-276, 2004.